THE JOURNAL OF PHYSICAL CHEMISTRY B

Article

pubs.acs.org/JPCB

Study of the Redox Properties of Singlet and Triplet Tris(2,2′-bipyridine)ruthenium(II) ($[Ru(bpy)_3]^{2+}$) in Aqueous Solution by Full Quantum and Mixed Quantum/Classical Molecular Dynamics Simulations

Polydefkis Diamantis, Jérôme Florian Gonthier,† Ivano Tavernelli, and Ursula Rothlisberger*

Laboratory of Computational Chemistry and Biochemistry, École Polytechnique Fédérale de Lausanne, CH-1015 Lausanne, Switzerland

Supporting Information

ABSTRACT: The oxidation of ground-state (singlet) and triplet $[Ru(bpy)_3]^{2+}$ were studied by full quantum-mechanical (QM) and mixed quantum/classical (QM/MM) molecular dynamics simulations. Both approaches provide reliable results for the redox potentials of the two spin states. The two redox reactions closely obey Marcus theory for electron transfer. The free energy difference between the two $[Ru(bpy)_3]^{2+}$ states amounts to 1.78 eV from both QM and QM/MM simulations. The two methods also provide similar results for the reorganization free energy associated with the transition from singlet to triplet $[Ru(bpy)_3]^{2+}$ (0.06 eV for QM and 0.07 eV for QM/MM). On the basis of single-point calculations, we estimate the entropic contribution to the free energy difference between singlet and triplet $[Ru(bpy)_3]^{2+}$ to be 0.27 eV, which is significantly greater than previously assumed (0.03 eV) and in contradiction with the assumption that the transition between these two states can be accurately described using purely energetic considerations. Employing a thermodynamic cycle involving singlet $[Ru(bpy)_3]^{2+}$, triplet $[Ru(bpy)_3]^{2+}$, and $[Ru(bpy)_3]^{3+}$, we calculated the triplet oxidation potential to be −0.62 V vs the standard hydrogen electrode, which is significantly different from a previous experimental estimate based on energetic considerations only (−0.86 V).

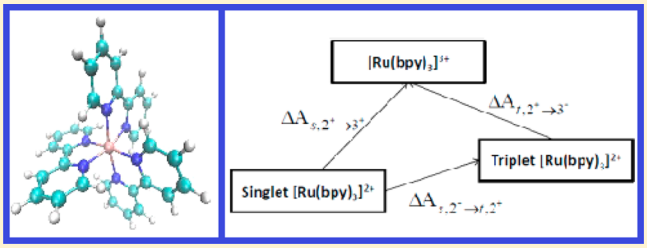

INTRODUCTION

Because of their unique chemical and photochemical properties (luminescence emission, reactive and long-lived excited states, and redox activity both in their ground and excited states[1,2]), ruthenium-based complexes are used in a wide variety of fields as parts of photovoltaics,[3] dye-sensitized solar cells,[4] electrochemiluminescence cells,[3,5] and light-emitting diodes (LEDs);[6] as photocatalysts[7] and redox agents for electron transfer reactions;[8,9] and for diagnostics.[10]

It is therefore no surprise that $[Ru(bpy)_3]^{2+}$, the prototype of these compounds, has been extensively studied experimentally[11−14] and computationally.[14−16] When photoexcited with visible light, this complex reaches a singlet metal-to-ligand charge transfer (^{1}MLCT) state and then undergoes a rapid transition (<100 fs[17,18]) to an excited triplet (^{3}MLCT) state.[13] This state has a lifetime of about 600 ns[19] and is particularly redox-active in solution, participating in electron transfer reactions.[20]

The redox activity of singlet and triplet $[Ru(bpy)_3]^{2+}$ has triggered a wide range of studies of their redox properties, in particular the standard oxidation potentials of these species. The singlet ground state of $[Ru(bpy)_3]^{2+}$ is the best characterized in this respect, with a well-established oxidation potential of 1.26 V[21] vs the standard hydrogen electrode (SHE). For the triplet state, however, the situation is not as clear. Although a value for the oxidation potential has been estimated (−0.86 V versus SHE),[1] it was obtained under the assumption that the Helmholtz free energy change for the transition from the ground state to the ^{3}MLCT state can be approximated by the corresponding minimum-to-minimum energy difference (2.15 eV in aqueous solution).[11] The only entropic term taken into consideration in this estimate is related to the spin change in going from singlet to triplet $[Ru(bpy)_3]^{2+}$, which amounts to only 0.03 eV.[11] This assumes that the structural changes and reorganization in transitions between the two states are negligible. The use of this approximation thus yields the standard oxidation potential of −0.86 V [resulting from 1.26 eV − (2.15 eV − 0.03 eV)] for the triplet state.

Crystallographic[22,23] and spectroscopic[13,22] studies are also in support of small structural changes in transitions between singlet and excited triplet $[Ru(bpy)_3]^{2+}$, thus indicating that their relative free energy difference might be energetically dominated.

A combined experimental and computational investigation of the fundamental redox properties (the reaction free energy and

Received: December 18, 2013
Revised: March 5, 2014
Published: March 10, 2014

the reorganization free energy of the oxidation reaction) of singlet $[Ru(bpy)_3]^{2+}$ in aqueous solution was recently performed by Blumberger and co-workers[14] using density functional theory-based Born−Oppenheimer (BO) molecular dynamics simulations with the Perdew−Burke−Ernzerhof (PBE) functional. Good agreement was observed between the computed values and the experimental data from photoelectron spectroscopy [1.20 eV (computed) vs 1.21 eV (experimental) for the reorganization free energy and 5.75 eV (computed) vs 5.60 eV (experimental) for the reaction free energy].

In the present work, we use a theoretical approach similar to the one applied in ref 14 in order to compute the redox properties of $[Ru(bpy)_3]^{2+}$ in both its ground state and its first excited triplet state using DFT with the BP86 functional, which is known to accurately reproduce geometries of transition-metal complexes in the gas phase.[24] In addition, we compare the results from full quantum-mechanical (QM) simulations to those obtained from mixed quantum/classical (QM/MM) simulations. The latter method has the advantage of being able to simulate larger system sizes but does not take possible polarization effects in the MM region into account. Because of this drawback, the ability of QM/MM simulations to provide accurate estimates of redox properties has been questioned.[25] The present work provides an opportunity to directly compare the performance of these two different simulation techniques for the same systems within an otherwise identical computational framework.

By comparing the reorganization free energies of the two reactions and by using a thermodynamic cycle involving singlet and triplet $[Ru(bpy)_3]^{2+}$ and $[Ru(bpy)_3]^{3+}$, we evaluate the reorganization free energy related to the singlet-to-triplet $[Ru(bpy)_3]^{2+}$ transition. We also investigate the nature of this transition and, in particular, attempt to determine its entropy contribution. We then use this information in combination with available experimental data in order to calculate the triplet-state oxidation potential, obtaining from both QM and QM/MM simulations a value of −0.62 V vs SHE, which is different from the previously suggested estimate of −0.86 V vs SHE.

THEORY

The redox properties and the free energy curves were determined through a theoretical approach originally suggested by Warshel,[26,27] who showed that the redox free energy change can be calculated from the distribution of the vertical energy gaps between the two states. This approach[28,29] has been successfully applied for the study of a series of different redox reactions in solution[14,29] and in protein environments.[30,31] Within this method, it is assumed that the Marcus theory of electron transfer[32−35] provides a valid description of the reaction, an assumption that can then be verified a posteriori by constructing the diabatic free energy curves of the two oxidation states. The most fundamental steps in the derivation of this computational scheme for redox potentials are briefly outlined below.

The redox reactions studied in the present work are schematically written in the form

$$R \rightarrow O + e^- \tag{1}$$

where R and O symbolize the reduced and oxidized states, respectively. The standard redox potential of the reaction shown in eq 1 is calculated through the expression

$$E_{0,R\rightarrow O} = -\frac{\Delta G_H - \Delta G_{R\rightarrow O}}{nF} \tag{2}$$

In eq 2, ΔG_H and $\Delta G_{R\rightarrow O}$ are the Gibbs free energy differences for the standard hydrogen electrode and the reaction shown in eq 1, respectively, n is the number of exchanged electrons, and F is Faraday's constant.

The following thermodynamic relation holds:

$$\Delta G_{R\rightarrow O} = \Delta A_{R\rightarrow O} + P\Delta V_{R\rightarrow O} \tag{3}$$

In eq 3, $\Delta A_{R\rightarrow O}$ is the Helmholtz free energy of oxidation, P is the pressure exerted on the compound, and V is its volume. In the case where the transition from one oxidation state to the other yields small structural changes, the second term in the right side of eq 3 can be neglected (i.e., $\Delta V_{R\rightarrow O} \approx 0$), and therefore, we can assume that $\Delta G_{R\rightarrow O} \approx \Delta A_{R\rightarrow O}$ for both redox reactions.

The Helmholtz free energy difference for the redox reaction shown in eq 1 is given by

$$\Delta A_{R\rightarrow O} = A_O - A_R = -k_B T \ln\left(\frac{Q_O}{Q_R}\right) \tag{4}$$

where Q_R and Q_O are the canonical partition functions of the reduced and oxidized states, respectively.

As previously stated, the information for computing $\Delta A_{R\rightarrow O}$ can be extracted from the distribution of the vertical energy gaps between the two states:

$$\Delta E_{R\rightarrow O}(\{R^N\}) = E_O(\{R^N\}) - E_R(\{R^N\}) \tag{5}$$

where $\{R^N\}$ stands for a given atomic configuration of the system. Depending on whether the reduced or oxidized state is the observer's reference state, $\Delta E_{R\rightarrow O}$ corresponds to the ionization energy or the electron affinity, respectively.

The vertical energy gaps can be inserted into eq 4, and it can then be proven[36] that

$$\Delta A_{R\rightarrow O} = -k_B T \ln\langle e^{-\Delta E_{R\rightarrow O}/k_B T}\rangle_R = k_B T \ln\langle e^{\Delta E_{R\rightarrow O}/k_B T}\rangle_O \tag{6}$$

This can be further simplified using Marcus theory,[32−35] in which it is assumed that the solvent responds linearly to a change in the charge of the solute. An automatic consequence is that the distributions of the vertical energy gaps for both the reduced and oxidized states will be Gaussian and that the standard deviations of the two distributions will be equal:

$$\sigma_R = \sigma_O = \sigma \tag{7}$$

The reorganization free energies of the reduced state (λ_R) and the oxidized state (λ_O) are directly determined from the respective variances and are therefore equal as well:

$$\lambda_R = \lambda_O = \frac{\sigma^2}{2k_B T} \tag{8}$$

If the validity of Marcus theory is assumed, eq 6 can be modified accordingly using Gaussian distributions as well as eq 7. The following relation is then obtained:

$$\Delta A_{R\rightarrow O} = \frac{1}{2}(\langle \Delta E_{R\rightarrow O}\rangle_R + \langle \Delta E_{R\rightarrow O}\rangle_O) \tag{9}$$

where $\langle \Delta E_{R\rightarrow O}\rangle_R$ and $\langle \Delta E_{R\rightarrow O}\rangle_O$ are the average ionization energy of the reduced state and the average electron affinity of the oxidized state, respectively.

dx.doi.org/10.1021/jp412395x | J. Phys. Chem. B 2014, 118, 3950−3959

From the distribution of $\Delta E_{R\to O}$ for the reduced and oxidized states, it is then possible to determine the diabatic free energy curves of the two states as predicted by Marcus theory. The reaction coordinate used for this procedure is a modified energy gap, labeled here as $\Delta E_{R\to O,\mu}$, given by the following expression:

$$\Delta E_{R\to O,\mu} = \Delta E_{R\to O} + \mu = \Delta E_{R\to O} - \Delta A_{R\to O} \tag{10}$$

To reach eq 10, the role of the electrode that provides the electron for the reaction shown in eq 1 has been assigned to a fictitious electron reservoir of electronic chemical potential μ. We then set $\mu = -\Delta A_{R\to O}$ in order to have zero total thermodynamic driving force $\Delta A_{R\to O,\mu}$, which is defined by the expression

$$\Delta A_{R\to O,\mu} = \Delta A_{R\to O} + \mu \tag{11}$$

A special property of this quantity is that if the value of the Helmholtz free energy in one oxidation state is given, the value in the other oxidation state can be directly calculated:[26,29]

$$\begin{aligned} &A_O(\Delta E_{R\to O,\mu}) - A_R(\Delta E_{R\to O,\mu}) = \Delta E_{R\to O,\mu} \\ &\Rightarrow -k_B T \ln\left[\frac{p_O(\Delta E_{R\to O,\mu})}{p_R(\Delta E_{R\to O,\mu})}\right] = \Delta E_{R\to O,\mu} \end{aligned} \tag{12}$$

The parabolic free energy curves can be expressed as

$$A_i(\Delta E_{R\to O,\mu}) = A_{\mu,i}^{\min} + \frac{1}{4\lambda}(\Delta E_{R\to O,\mu} - \Delta E_{R\to O,\mu}^{\min})^2 \tag{13}$$

In eq 13, $A_{\mu,i}^{\min}$ and $\Delta E_{R\to O,\mu}^{\min}$ are the minimum free energy of state i and the energy gap for which this minimum is encountered, respectively.

By definition, the following expression for the reorganization free energy of state i can be written:

$$\lambda_i = A_i(\Delta E_{\mu,j}^{\min}) - A_i(\Delta E_{\mu,i}^{\min}) \tag{14}$$

where the index j refers to the other oxidation state. Addition of the expressions for λ_R and λ_O from eq 14, combined with eq 8 and the Gaussian energy gap distributions, provides the following relation for the calculation of the reorganization free energy:

$$\lambda = \frac{1}{2}(\langle \Delta E_{R\to O}\rangle_R - \langle \Delta E_{R\to O}\rangle_O) \tag{15}$$

METHODS

QM Simulations. Tris(2,2′-bipyridine)ruthenium(II) (Figure 1A) was solvated in a periodic cubic box with a side length of 15.84 Å (Figure 1B) containing 104 TIP3P[37] water molecules. The system was first equilibrated classically for 16 ns at 300 K and 1 atm using the Amber 11 package[38] with the general Amber force field (GAFF).[39] During the equilibration, strict positional restraints were applied to the atoms of the ruthenium complex using a force constant of 500 kcal mol^{-1} Å^{-2}. Force field parameters for the latter were taken from a previous work on $[Ru(bpy)_3]^{2+/3+}$.[40]

A QM equilibration at 300 K (*NVT* ensemble) was subsequently performed for each system ($[Ru(bpy)_3]^{2+/3+}$ positional restraints were removed), starting with Born–Oppenheimer molecular dynamics (BO MD) and then switching to Car–Parrinello molecular dynamics (CP MD)[41] using a fictitious electron mass of 400 au. For $[Ru(bpy)_3]^{2+}$, CP MD was performed for 1.8 ps, while for the oxidized state the same stage lasted 3 ps. This was succeeded by 4.5 ps long production phases performed in the *NVE* ensemble using CP MD and a time step of 4 au (0.096 fs). All of the full QM simulations were performed with the CPMD program[42] using a plane-wave basis set with a cutoff of 75 Ry and applying norm-conserving Troullier–Martins (MT) pseudopotentials[43] for the interactions of the valence electrons with the ionic cores. The systems were described at the DFT/BP86[44,45] level of theory. The frames to be analyzed were extracted every 10 fs from each trajectory.

QM/MM Simulations. The system setup for the QM/MM simulations was chosen as in ref 40. The total system consisted of the Ru complex, two Cl^- counterions, and 3298 water molecules in a periodic cubic box with a length of 46.66 Å (Figure 1C).

The Ru complex was treated at the QM level using DFT/BP86, while the water and the counterions were described classically with the TIP3P and GAFF force fields, respectively. The QM/MM interface of the CPMD code was used for the simulations, in which the MM region is simulated by the GROMOS code.[46] The coupling between the QM and MM regions was described by the explicit coupling scheme introduced by Rothlisberger and co-workers.[47,48] For the QM region (enclosed in a cubic box with a side length of 18 Å), we applied the same plane-wave basis set and MT pseudopotentials as in the full QM simulations.

For all three states of the complex (singlet $[Ru(bpy)_3]^{2+}$, triplet $[Ru(bpy)_3]^{2+}$, and $[Ru(bpy)_3]^{3+}$), the system was initially equilibrated at 300 K, starting with BO MD and then switching to CP MD. The equilibration was followed by a 5 ps production run with CP MD in the *NVE* ensemble with a time step of 4 au and a fictitious electron mass of 400 au. Sampling took place every 10 fs of each trajectory.

Static QM Calculations. For the sake of comparison, single-point calculations of the vertical energy gaps between singlet/triplet $[Ru(bpy)_3]^{2+}$ and doublet $[Ru(bpy)_3]^{3+}$ were also performed with the Gaussian 09 (G09) package[49] using the same DFT/BP86 description as for the dynamic simulations. The starting geometry for the complex was provided by a random frame from the QM simulations and was initially optimized. The electrons were described by a TZVP basis set except for the electrons of the ruthenium atom, which were described by the LANL2DZ basis set. To assess the effect of solvent on the vertical energy gaps, calculations were performed in vacuum as well as with implicit solvent using the polarizable continuum model (PCM)[50−52] for water, with a dielectric constant of 80.

The solvent response upon changing the oxidation state can be divided into fast and slow components, corresponding to the solvent's electronic and nuclear responses, respectively. When the standard PCM model is applied in both redox states, both

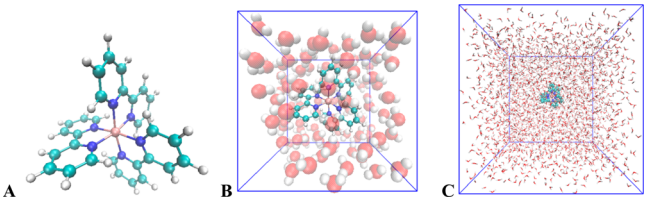

Figure 1. (A) Structure of $[Ru(bpy)_3]^{2+/3+}$ and (B, C) the system in the (B) full QM and (C) QM/MM simulations.

dx.doi.org/10.1021/jp412395x | J. Phys. Chem. B 2014, 118, 3950−3959

components would be taken into consideration. The resulting energy difference would therefore not correspond to a vertical energy gap. To address this issue, we employed the nonequilibrium PCM protocol implemented in G09.[53,54] In this scheme, the standard PCM model is used to optimize the geometry of the solute in the initial state. In a subsequent SCF step on the optimized geometry, information is saved for the fast and slow responses of the solvent. In the final step, the energy of the final state is calculated, while only the fast response of the solvent is taken into consideration. The nonequilibrium PCM scheme has been successfully applied in the calculation of the vertical ionization energies of imidazole (neutral[55] and protonated[56]) and of DNA building blocks.[57]

DATA ANALYSIS

General Procedure for the Analysis of the Trajectories. The driving force and the reorganization free energy of the redox reactions were derived from the vertical energy gap distributions as described in eqs 9 and 15. The distributions of $\Delta E_{R\rightarrow O}$ were then converted to distributions of $\Delta E_{R\rightarrow O,\mu}$. From those, the respective Helmholtz free energy curves were constructed using the equation

$$A(\Delta E_{R\rightarrow O,\mu}) = -k_B T \ln[p(\Delta E_{R\rightarrow O,\mu})] \quad (16)$$

For state i of each reaction (where i is either R or O), additional points were calculated from the distribution of $\Delta E_{i\rightarrow j,\mu}$ of the opposite oxidation state j using eq 12.

Corrections Applied to the Calculated Values of the Redox Properties. Because of the finite size of the periodic simulation cells and the way in which charge neutrality is enforced when the system is charged, it is necessary to apply corrections to the resulting values. These correction terms were obtained from the study of $[Ru(bpy)_3]^{2+/3+}$ by Blumberger and co-workers.[14] Even though this work involved only ground-state $[Ru(bpy)_3]^{2+}$, these corrections can be equally applied to the excited triplet state.

The correction terms that should be used for $\Delta A_{R\rightarrow O}$ and $\lambda_{R\rightarrow O}$ are presented in the following two equations:

$$\Delta A_{R\rightarrow O} = \Delta A_{R\rightarrow O,calc} + C_{\Delta A,1} + C_{\Delta A,2} \quad (17)$$

$$\lambda_{R\rightarrow O} = \lambda_{R\rightarrow O,calc} + C_{\lambda,1} \quad (18)$$

The correction terms with "1" in the subscript are associated with the box size correction, while $C_{\Delta A,2}$ compensates for the shift induced in $\Delta A_{R\rightarrow O}$ by the different neutralizing background charges of the periodic box in the reduced and oxidized states of the complex. Such a term is not needed for the reorganization free energy, as the total charge of the system remains unchanged upon structural reorganization.

When a system is simulated in a periodic box, part of the outer sphere is not included, and hence, the corresponding contribution to $\Delta A_{R\rightarrow O}$ is missed. For our systems, $C_{\Delta A,1}$ can be determined from its variation as a function of the reciprocal of the box volume (given in graph 9C in Figure 9 of ref 14), provided by the following linear equation:

$$C_{\Delta A,1} = \alpha_1 \frac{1}{V_{box}} + \beta_1 \quad (19)$$

where V_{box} is the volume of the periodic box. The coefficients α_1 and β_1 were determined by linear regression with R^2 = 0.9868.

The need for $C_{\Delta A,2}$ arises from the difference between the theoretical and experimental definitions of the zero electrostatic potential (ZEP) reference. In theory, neutrality for a given periodic cell is enforced in the Ewald summation scheme through the equation[58−60]

$$\int_{V_{cell}} \phi(\mathbf{r})\, d^3\mathbf{r} = 0 \quad (20)$$

where $\phi(\mathbf{r})$ is the Ewald potential and V_{cell} is the volume of the periodic simulation box. When the system is not neutral, eq 20 enforces charge neutrality by introducing a background charge. Consequently, this gives rise to nonphysical interactions between the background charges of periodic images. In the experiment, the ZEP reference is located at an infinite distance from a certain sample of the aqueous solution. Clearly, the different charges of $[Ru(bpy)_3]^{2+/3+}$ in each state (reduced/oxidized) yield different background charges. For a finite box size, the nonphysical interactions do not cancel each other in the calculation of $\Delta A_{R\rightarrow O}$. For sufficiently large boxes, $C_{\Delta A,2}$ is independent of the box size and depends only on the solvent.[61] It can thus be estimated for a certain box size by subtracting the experimental Gibbs free energy difference (ΔG_{exp}) of a reference reaction from the computed value (ΔG_{calc}):

$$C_{\Delta A,2} = \Delta G_{calc} - \Delta G_{exp} \quad (21)$$

A simple reference reaction for this purpose is proton hydration, for which ΔG_{exp} has been determined.[62]

Finally, the reorganization free energy also has to be corrected in order to take the missing long-range outer-sphere reorganization into account. $C_{\lambda,1}$ for our $[Ru(bpy)_3]^{2+/3+}$ systems was again taken from ref 14, where the calculated reorganization free energy was determined as a function of the square root of the reciprocal of the box side length (graph 9A in Figure 9 of ref 14):

$$C_{\lambda,1} = \alpha_2 \sqrt{\frac{1}{L_{box}}} + \beta_2 \quad (22)$$

in which L_{box} is the box side length and α_2 and β_2 were determined with R^2 = 0.9996.[14] $C_{\lambda,1}$ in the dilution limit can be extracted via an extrapolation.

Corrections for the Values Obtained via QM Simulations. From graph 9C of ref 14, the correction to the redox free energy difference due to finite size effects, $C_{\Delta A,1}$, amounts to 0.35 ± 0.01 eV for a box with an edge length of 15.84 Å. In regard to $C_{\Delta A,2}$, applying eq 21 for proton hydration yields a value of 3.70 ± 0.22 eV[61,63] for simulation with a 10 Å periodically repeated cubic water box using the BLYP functional.[45,64] With respect to the reorganization free energy, for a box of 15.84 Å side length, a value of $C_{\lambda,1}$ equal to 1.04 ± 0.2 meV was obtained from graph 9A of ref 14.

Corrections for the Values Obtained via QM/MM Simulations. The correction terms $C_{\Delta A,1}$ and $C_{\Delta A,2}$ were evaluated with completely different full QM computational setups, and their application to the QM/MM simulations is considered with caution. However, for the QM/MM box size of 46.66 Å used here, which is close to infinite dilution, the outer-sphere contribution to the driving force appears to be negligible,[14] and therefore $C_{\Delta A,1} \approx 0$. For the same reason, $C_{\Delta A,2}$ is also approximately equal to 0.

Neutralization of the $[Ru(bpy)_3]^{3+}$ system could be achieved with the addition of a third explicit Cl^- ion or with a compensating background charge. Either approach should be

dx.doi.org/10.1021/jp412395x | J. Phys. Chem. B 2014, 118, 3950−3959

accompanied by a modification of the classical topology file. In addition, there would be limitations in both approaches. In the first case, the vertical energy gap would strongly depend on the position of the counterion and the degree to which the resulting geometry is in an equilibrium configuration. Employment of the second approach would demand a correction term for the compensating background charge to be evaluated. Because of these drawbacks, neither option was selected. From a theoretical point of view, even though several correction schemes exist[65−67] and could be employed, we used the fact that electron ionization and electron attachment are exactly opposite processes. This implies that they will have opposite correction terms, defined here as CT and −CT, respectively. These terms cancel each other out in the calculation of $\Delta A_{R\rightarrow O}$ (eq 9) but not in the calculation of the reorganization free energy (eq 15).

An estimate of $\lambda_{s,2^+\rightarrow t,2^+}$, the relative difference in the reorganization free energies of singlet and triplet $[Ru(bpy)_3]^{2+}$, can also be obtained by considering its definition:

$$\lambda_{s,2^+\rightarrow t,2^+} = \lambda_{t,2^+\rightarrow 3^+} - \lambda_{s,2^+\rightarrow 3^+} \quad (23)$$

The Gaussian nature of the vertical energy gap distributions can also be determined, as each is just shifted by its correction term (CT and −CT, respectively). In the following, we give only quantities for which this correction cancels out.

RESULTS

Structural Properties. In order to equate $\Delta A_{R\rightarrow O}$ with $\Delta G_{R\rightarrow O}$ and apply eq 2, we analyzed the differences in bond lengths for the different oxidation states. For this purpose, we used (i) the G09-optimized geometries of singlet $[Ru(bpy)_3]^{2+}$, triplet $[Ru(bpy)_3]^{2+}$, and $[Ru(bpy)_3]^{3+}$ in the gas phase and in implicit solvent (see Figures 1A,B and 2A,B in the Supporting Information) and (ii) the finite-temperature configurations obtained in the full QM simulations at 300 K. The results are summarized in Table 1.

It is evident that for each bond type, the average bond lengths of all three states are very close, with the changes being smaller than the typical thermal fluctuations. These findings indicate that the inner-sphere contribution to the total reorganization free energy is small, in agreement with the explicit QM calculations of the reorganization free energies of the singlet and triplet $[Ru(bpy)_3]^{2+}$ oxidation reactions, for which 87.4% and 83.2%, respectively, turn out to be due to outer-sphere contributions $[(C_{\lambda,1}/\lambda_{R\rightarrow O})\cdot 100\%$, where because of the small size of the QM box, $C_{\lambda,1}$ corresponds to the outer-sphere contribution). It can therefore be deduced that the effects of the change in oxidation state on the pressure exerted on the complex and on its volume are most probably negligible. We thus assume that $P\Delta V_{R\rightarrow O} \approx 0$ and therefore, from eq 3, that $\Delta G_{R\rightarrow O} \approx \Delta A_{R\rightarrow O}$ for both redox reactions.

QM Simulations. The distributions of the vertical energy gaps (see the graphs reported in the Supporting Information) were determined using a bin width of 0.05 eV. The $\Delta E_{R\rightarrow O} - \langle \Delta E_{R\rightarrow O}\rangle$ distributions were plotted for the oxidations of both singlet and triplet $[Ru(bpy)_3]^{2+}$.

For singlet $[Ru(bpy)_3]^{2+}$, the average ionization energy is equal to 1.46 ± 0.01 eV, while the average electron affinity has a value of 1.17 ± 0.01 eV. From eq 9, the redox free energy difference for the reaction, $\Delta A_{s,2^+\rightarrow 3^+,calc}$, is thus 1.32 eV (with a statistical uncertainty lower than 0.01 eV). Substituting the average ionization energy and electron affinity into eq 15, we obtain a value of 0.15 eV (with a statistical uncertainty lower than 0.01 eV) for the corresponding reorganization free energy, $\lambda_{s,2^+\rightarrow 3^+,calc}$.

Table 1. Average Bond Lengths of the Optimized Geometries of $[Ru(bpy)_3]^{2+}$ and $[Ru(bpy)_3]^{3+}$ in the Gas Phase and under Implicit (PCM) Solvation (ε = 80) and from the Production Phases of the QM Simulations with the Corresponding Thermal Fluctuations

	average bond length (Å)		
bond type	singlet $[Ru(bpy)_3]^{2+}$	triplet $[Ru(bpy)_3]^{2+}$	$[Ru(bpy)_3]^{3+}$
G09, Gas Phase			
Ru−N	2.091	2.090	2.103
N−C	1.364	1.371	1.365
C−C (between pyridine rings)	1.471	1.451	1.470
C−C (in a pyridine ring)	1.397	1.398	1.397
C−H	1.090	1.090	1.091
G09, Implicit Solvation			
Ru−N	2.086	2.088	2.096
N−C	1.363	1.369	1.362
C−C (between pyridine rings)	1.470	1.450	1.467
C−C (in a pyridine ring)	1.396	1.397	1.395
C−H	1.090	1.090	1.089
CP MD at 300 K			
Ru−N	2.069 ± 0.051	2.073 ± 0.050	2.079 ± 0.049
N−C	1.365 ± 0.030	1.370 ± 0.027	1.364 ± 0.024
C−C (between pyridine rings)	1.468 ± 0.032	1.451 ± 0.027	1.466 ± 0.025
C−C (in a pyridine ring)	1.396 ± 0.026	1.397 ± 0.023	1.395 ± 0.022
C−H	1.092 ± 0.023	1.091 ± 0.018	1.092 ± 0.021

As far as the triplet $[Ru(bpy)_3]^{2+}$ oxidation reaction is concerned, the average values of $\langle \Delta E_{R\rightarrow O}\rangle_R$ and $\langle \Delta E_{R\rightarrow O}\rangle_O$ are −0.25 ± 0.01 and −0.67 ± 0.01 eV, respectively, yielding a Helmholtz free energy difference, $\Delta A_{t,2^+\rightarrow 3^+,calc}$, equal to −0.46 eV (with a statistical uncertainty lower than 0.01 eV). The reorganization free energy, $\lambda_{t,2^+\rightarrow 3^+,calc}$, was calculated to be 0.21 eV (with a statistical uncertainty lower than 0.01 eV).

Taking the correction terms for the QM simulations into account, the final values of the driving forces for the singlet and triplet oxidations become 5.37 ± 0.22 and 3.59 ± 0.22 eV, respectively, while the corresponding reorganization free energies are 1.19 and 1.25 eV (with a statistical uncertainty lower than 0.01 eV).

The corresponding reconstructed Helmholtz free energy curves (according to eqs 16 and 12) are shown in Figure 2A,B for the singlet and triplet state oxidations, respectively. They are parabolas to a very good approximation, with coefficients of determination (R^2) of 0.995 and 0.994 for the singlet $[Ru(bpy)_3]^{2+}$ redox half reaction, and of 0.996 and 0.999 for the triplet $[Ru(bpy)_3]^{2+}$ redox half reaction.

In order to determine λ, $\Delta E^{min}_{R\rightarrow O,\mu}$, and $A^{min}_{\mu,i}$ for the singlet and triplet $[Ru(bpy)_3]^{2+}$ oxidations, eq 13 can be rearranged as follows:

dx.doi.org/10.1021/jp412395x | J. Phys. Chem. B 2014, 118, 3950−3959

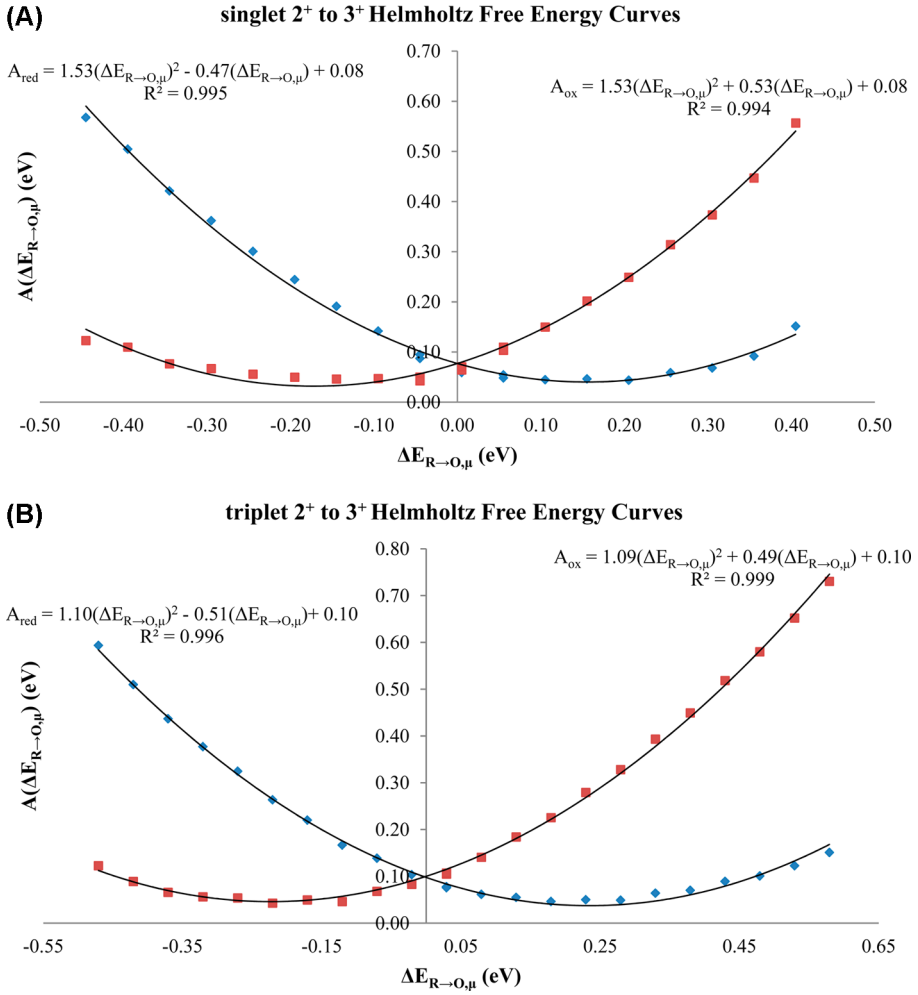

Figure 2. Free energy curves of (A) singlet or (B) triplet $[Ru(bpy)_3]^{2+}$ (A_{red}, blue points) and $[Ru(bpy)_3]^{3+}$ (A_{ox}, red points) from full QM simulations.

$$A_i(\Delta E_{R\rightarrow O,\mu}) = \frac{1}{4\lambda}(\Delta E_{R\rightarrow O,\mu})^2 - \frac{\Delta E^{min}_{R\rightarrow O,\mu}}{2\lambda}\Delta E_{R\rightarrow O,\mu} + \left[A^{min}_{\mu,i} + \frac{(\Delta E^{min}_{R\rightarrow O,\mu})^2}{4\lambda}\right] \quad (24)$$

The results are reported in Table 2.

QM/MM Simulations. As in the case of the full QM simulations, the $\Delta E_{R\rightarrow O} - \langle \Delta E_{R\rightarrow O}\rangle$ distributions for the oxidations of singlet and triplet $[Ru(bpy)_3]^{2+}$ were determined using a bin width of 0.05 eV (see the graphs reported in the Supporting Information).

Table 2. Calculated Values of Reorganization Free Energies, Minimum Free Energies, and Their Corresponding Vertical Energy Gaps from Full QM Simulations

Singlet $[Ru(bpy)_3]^{2+}$ Oxidation Reaction						
λ_R (eV)	λ_O (eV)	$\lambda_{s,2^+\rightarrow 3^+}$ (eV)	$\Delta E^{min}_{\mu,s,2^+}$ (eV)	$\Delta E^{min}_{\mu,3^+}$ (eV)	$A^{min}_{\mu,s,2^+}$ (eV)	$A^{min}_{\mu,3^+}$ (eV)
0.164	0.164	0.164	0.156	−0.172	0.040	0.032
Triplet $[Ru(bpy)_3]^{2+}$ Oxidation Reaction						
λ_R (eV)	λ_O (eV)	$\lambda_{t,2^+\rightarrow 3^+}$ (eV)	$\Delta E^{min}_{\mu,t,2^+}$ (eV)	$\Delta E^{min}_{\mu,3^+}$ (eV)	$A^{min}_{\mu,t,2^+}$ (eV)	$A^{min}_{\mu,3^+}$ (eV)
0.227	0.230	0.229	0.234	−0.223	0.037	0.046

From the distributions for the singlet oxidation, the average ionization energy and the average electron affinity are 6.97 ± 0.01 and 4.95 ± 0.01 eV, respectively. Therefore, the computed driving force of this reaction, $\Delta A_{s,2^+\rightarrow 3^+,calc}$, is 5.96 ± 0.22 eV (including the statistical uncertainty for $C_{\Delta A,1}$ and $C_{\Delta A,2}$).

For the triplet oxidation, we obtained $\langle \Delta E_{R\rightarrow O}\rangle_R$ = 5.25 ± 0.01 eV and $\langle \Delta E_{R\rightarrow O}\rangle_O$ = 3.10 ± 0.01 eV. They lead to a Helmholtz free energy difference of $\Delta A_{t,2^+\rightarrow 3^+,calc}$ = 4.18 ± 0.22 eV (including the statistical uncertainty for $C_{\Delta A,1}$ and $C_{\Delta A,2}$).

Gaussian Calculations. The calculated values of the vertical ionization potentials and electron affinities are reported in Table 3. By subtraction of the vertical ionization energies of triplet $[Ru(bpy)_3]^{2+}$ from the vertical ionization energies of its ground state, the adiabatic energy differences between the two states were calculated to be 2.08 and 2.05 eV for the species in the gas phase and in solution, respectively. These results, when compared with the QM/MM averages of the vertical energy gaps, confirm our argument that the correction terms for the ionization energies and electron affinities should be of equal absolute value but opposite sign.

DISCUSSION

Comparison with the Literature. The experimental value of the vertical ionization energy of singlet $[Ru(bpy)_3]^{2+}$ is 6.81

dx.doi.org/10.1021/jp412395x | J. Phys. Chem. B 2014, 118, 3950−3959

Table 3. G09-Calculated Vertical Energy Gaps[a]

singlet $[Ru(bpy)_3]^{2+}$ oxidation reaction				triplet $[Ru(bpy)_3]^{2+}$ oxidation reaction			
PCM		gas phase		PCM		gas phase	
$[Ru(bpy)_3]^{2+}$ IE	6.75	$[Ru(bpy)_3]^{2+}$ IE	12.35	$[Ru(bpy)_3]^{2+}$ IE	4.70	$[Ru(bpy)_3]^{2+}$ IE	10.28
$[Ru(bpy)_3]^{3+}$ EA	5.14	$[Ru(bpy)_3]^{3+}$ EA	12.27	$[Ru(bpy)_3]^{3+}$ EA	3.11	$[Ru(bpy)_3]^{3+}$ EA	10.16

[a]IE stands for ionization energy and EA for electron affinity (in eV).

eV.[14] Our computed value, 6.75 eV (Table 3), is in very good agreement.

An experimental value of 5.60 eV for $\Delta A_{R\rightarrow O}$ of the ground-state $[Ru(bpy)_3]^{2+}$ oxidation reaction in solution was determined in ref 14. Our QM and QM/MM values both compare well with this value. Our QM value for $\Delta A_{R\rightarrow O}$ (5.37 eV) is shifted by 0.23 eV from the experimental estimate. This is within the usual error of the BP86 functional for ionization energies and electron affinities (ca. 0.2 eV),[68] and therefore, our result is in good agreement with the experimental value. The QM/MM value for $\Delta A_{s,2^+\rightarrow 3^+}$ (5.96 eV) is slightly further away from the experimental value.

An experimental estimate of the reorganization free energy associated with the singlet oxidation ($\lambda_{s,2^+\rightarrow 3^+}$) has also been determined,[14] which amounts to 1.21 eV. We calculated a corresponding QM value of 1.19 eV, in excellent agreement with this estimate as well as with the value determined using the PBE functional (1.20 eV[14]).

The triplet-state calculations were performed using the same protocol as used for the singlet state. We therefore expect the same accuracy, even though a direct comparison with experiments is not possible in this case because of the lack of direct experimental data.

Applicability of Marcus Theory. The analysis of the QM results confirms that both reactions can be accurately described within Marcus theory. The distributions of the vertical energy gaps are to a very good approximation Gaussian for both the singlet and triplet $[Ru(bpy)_3]^{2+}$ oxidation states. For each reaction, the standard deviations of the ionization energy and electron affinity distributions are in very good agreement (singlet oxidation, 0.10 and 0.11 eV; triplet oxidation, 0.13 and 0.11 eV). In addition, the free energy curves obtained from both methods are intersecting parabolas with R^2 values close to unity. Moreover, the reorganization free energies obtained from the curves perfectly match their respective values determined from the analysis of the vertical energy distributions. The conclusion that singlet $[Ru(bpy)_3]^{2+}$ oxidation can be described by the Marcus theory of electron transfer is in agreement with recent findings,[14] while to the best of our knowledge, the present work is the first to show that the same theory also applies to the triplet oxidation state.

The QM/MM-determined standard deviations of the vertical energy gap distributions are larger than the equivalent QM values as a consequence of more extensive sampling due to the larger box size. Also in this case, the values both for the singlet $[Ru(bpy)_3]^{2+}$ oxidation (0.28 and 0.25 eV) and the triplet $[Ru(bpy)_3]^{2+}$ oxidation (0.30 and 0.25 eV) are very close, showing again that Marcus theory is valid.

Free Energy Difference between Ground-State and Triplet $[Ru(bpy)_3]^{2+}$ and Estimation of $E°$ for Triplet $[Ru(bpy)_3]^{2+}$. From the calculated Helmholtz free energy differences for the singlet and triplet $[Ru(bpy)_3]^{2+}$ oxidations in solution, it is also possible to calculate a value for the relative difference between the Helmholtz free energies of singlet and triplet $[Ru(bpy)_3]^{2+}$, $\Delta A_{s,2^+\rightarrow t,2^+}$, using the following formula:

$$\Delta A_{s,2^+\rightarrow t,2^+} = \Delta A_{s,2^+\rightarrow 3^+} - \Delta A_{t,2^+\rightarrow 3^+} \quad (25)$$

Application of eq 25 leads to an identical value of 1.78 eV for $\Delta A_{s,2^+\rightarrow t,2^+}$, from both the QM and QM/MM simulations.

The values of the relative difference in reorganization free energy, $\lambda_{s,2^+\rightarrow t,2^+}$, obtained from the QM and QM/MM simulations (0.06 and 0.07 eV, respectively) both reconfirm that only a small reorganization occurs in transitions between the ground state and the triplet state, in agreement with the experimental measurements. Adding to the evidence of structural similarity is the fact that upon solvation the ionization energies of the two states undergo practically identical shifts (singlet reduced by 5.60 eV and triplet by 5.58 eV; Table 3). Moreover, the same is true for the electron affinities (7.13 and 7.05 eV respectively; Table 3). Finally, the small decrease in the adiabatic energy gap ($\Delta U_{s,2^+\rightarrow t,2^+}$) upon solvation (0.04 eV) also indicates structural similarity between singlet and triplet $[Ru(bpy)_3]^{2+}$.

However, in order to accurately estimate the redox potential of the triplet oxidation, it is necessary to make a deeper investigation about the exact character of the difference between the two states. We chose a single BP86 value of $\Delta U_{s,2^+\rightarrow t,2^+}$ for this purpose. From our implicit solvent calculations performed with G09, we obtain $\Delta U_{s,2^+\rightarrow t,2^+}$ = 2.05 eV, which is reasonably close to the experimental value of 2.15 eV. Subtraction of $\Delta A_{s,2^+\rightarrow t,2^+}$ from $\Delta U_{s,2^+\rightarrow t,2^+}$ provides a way to estimate the entropy change at a given temperature T:

$$T\Delta S_{s,2^+\rightarrow t,2^+} = \Delta U_{s,2^+\rightarrow t,2^+} - \Delta A_{s,2^+\rightarrow t,2^+} \quad (26)$$

From eq 26, we get $\Delta S_{s,2^+\rightarrow t,2^+}$ = 0.90 meV/K at T = 300 K. This outcome further confirms the notion that the reorganization in transitions between singlet and triplet $[Ru(bpy)_3]^{2+}$ is very small.

Its impact on the free energy change at 300 K, however, is $T\Delta S_{s,2^+\rightarrow t,2^+}$ = 0.27 eV. This result is in contrast with the value of 0.03 eV assumed by Sutin et al.,[11] fully attributed to the spin change, on the basis of which it was considered that the free energy difference between singlet and triplet $[Ru(bpy)_3]^{2+}$ is practically equal to the energy difference. This finding therefore provides an indication that besides the spin change ($T\Delta S$ = 0.03 eV), there are additional factors contributing to the entropy change of the singlet-to-triplet transition in $[Ru(bpy)_3]^{2+}$. To address this question, we investigated the difference in the structural organization of water molecules around singlet and triplet $[Ru(bpy)_3]^{2+}$. Using the Ru−O radial pair distribution functions (where O is the water's oxygen atom), and their integrals, we determined the differences in the solvent's structural reorganization upon oxidation of singlet and triplet $[Ru(bpy)_3]^{2+}$. This analysis (see Figures 5−8 in the Supporting Information) shows that the difference in solvent reorganization is indeed significant. In agreement with previous computational studies,[15,16] we found that in both singlet and triplet $[Ru(bpy)_3]^{2+}$, the first solvation shell is composed of intercalated meandering chains of H-bonded water molecules (Figure 3). Integration of the Ru−O distribution functions

dx.doi.org/10.1021/jp412395x | J. Phys. Chem. B 2014, 118, 3950−3959

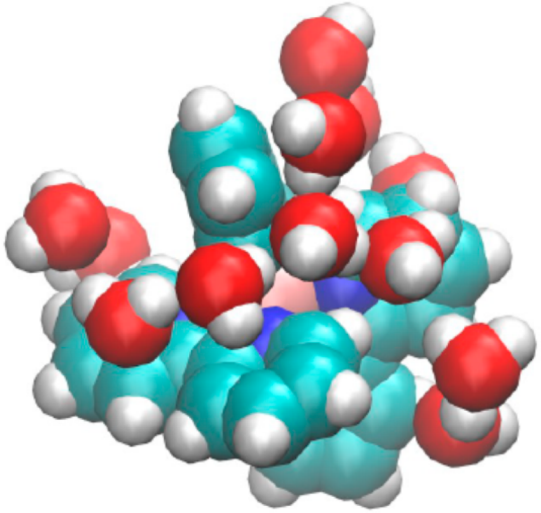

Figure 3. The first solvation shell of triplet $[Ru(bpy)_3]^{2+}$, consisting of water molecules with atoms within 6.1 Å of Ru. Color assignments: light pink, Ru; blue, N; green, C; white, H; red, O. This snapshot was obtained from our full QM trajectory.

revealed that the first solvation shell of the triplet state contains 2.0 more water molecules than that of the singlet (8.2 vs 6.2). The arrangement of water molecules in the outer solvation shells compensates for this difference (Figure 8 in the Supporting Information). The same changes are also reflected in the rearrangement of water molecules upon singlet and triplet oxidation (Figure 7 in the Supporting Information). The changes in the number of water molecules in the first solvation shell are 1.6 and −0.4 upon singlet and triplet oxidation, respectively. This finding, in combination with the small inner-sphere reorganization observed in transitions between the two states, shows that a major part of the entropy change during the transition originates from the structural reorganization of water in close proximity to the complex.

From the result for $\Delta A_{s,2^+\rightarrow t,2^+}$, the standard oxidation potential of triplet $[Ru(bpy)_3]^{2+}$, $E^\circ_{t,2^+\rightarrow 3^+}$, can be estimated with the help of the thermodynamic cycle displayed in Figure 4.

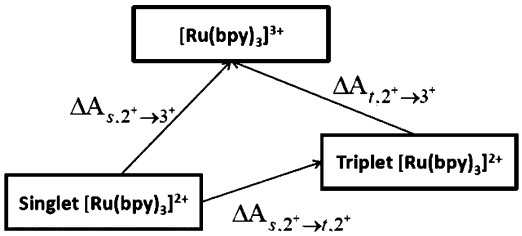

Figure 4. Thermodynamic cycle involving singlet $[Ru(bpy)_3]^{2+}$, triplet $[Ru(bpy)_3]^{2+}$, and $[Ru(bpy)_3]^{3+}$.

On the basis of this thermodynamic cycle, the non-negligible entropy change that we calculated indicates that the true value of $E^\circ_{t,2^+\rightarrow 3^+}$ is sizably different from the one reported in the literature (−0.86 V).[1] An estimate of $E^\circ_{t,2^+\rightarrow 3^+}$ can be obtained by converting the experimental value of $\Delta U_{s,2^+\rightarrow t,2^+}$ (2.15 eV) to $\Delta A_{s,2^+\rightarrow t,2^+}$. Using eq 26, we get $\Delta A_{s,2^+\rightarrow t,2^+} = (2.15 - 0.27)$ eV = 1.88 eV. Equation 25 can be rewritten as follows:

$$\Delta A_{s,2^+\rightarrow t,2^+} = (\Delta A_{s,2^+\rightarrow 3^+} - \Delta G_H) - (\Delta A_{t,2^+\rightarrow 3^+} - \Delta G_H) \quad (27)$$

Dividing eq 27 by nF and taking the definition of the standard redox potential from eq 2 into consideration gives

$$E^\circ_{t,2^+\rightarrow 3^+} = E^\circ_{s,2^+\rightarrow 3^+} - \frac{\Delta A_{s,2^+\rightarrow t,2^+}}{nF} \quad (28)$$

From eq 28, $E^\circ_{t,2^+\rightarrow 3^+}$ amounts to −0.62 V, in contrast to the previous estimate of −0.86 V. The fact that this result was obtained from both simulation protocols (full QM and QM/MM) clearly shows that it is by no means safe to estimate $E^\circ_{t,2^+\rightarrow 3^+}$ by neglecting the solvent's contribution to $T\Delta S_{s,2^+\rightarrow t,2^+}$.

CONCLUSION

QM and QM/MM density functional molecular dynamics simulations of the oxidation of singlet $[Ru(bpy)_3]^{2+}$ to $[Ru(bpy)_3]^{3+}$ yield Helmholtz free energy differences of oxidation for the singlet state ($\Delta A_{s,2^+\rightarrow 3^+}$) that are close to the experimental estimate. The oxidation of the excited triplet state of $[Ru(bpy)_3]^{2+}$ was studied using exactly the same simulation protocol, and therefore, the QM and QM/MM free energy differences evaluated for this half-reaction should be equally reliable.

Concerning the reorganization free energies, $\lambda_{R\rightarrow O}$, we obtained QM estimates of 1.19 and 1.25 eV for the singlet and triplet oxidations, respectively, the former being in excellent agreement with the available experimental value. In addition, the small difference between $\lambda_{s,2^+\rightarrow 3^+}$ and $\lambda_{t,2^+\rightarrow 3^+}$, which was also observed in the QM/MM simulations (0.07 eV), confirms the experimental evidence for structural similarity between the two states.

The present work reveals that QM/MM simulations can predict Helmholtz free energy changes for redox half-reactions that are in good agreement with values obtained from full QM simulations. The two simulation types also provide equally solid evidence that both reactions are accurately described by Marcus theory. Concerning the singlet-to-triplet transition, they yield an exactly identical term for the entropy change ($T\Delta S$ = 0.27 eV) that disagrees with the previously assumed estimate (0.03 eV).[11] This leads to a standard oxidation potential of −0.62 V for triplet $[Ru(bpy)_3]^{2+}$. This value is 0.24 V larger than the previously estimated value, which, as stated before, does not account for the solvent's entropic contribution to the free energy difference between singlet and triplet $[Ru(bpy)_3]^{2+}$.

ASSOCIATED CONTENT

Supporting Information

Figures showing the optimized geometries of the complex both in vacuum and under implicit solvation as well as the vertical energy gap distributions ($\Delta E_{R\rightarrow O} - \langle \Delta E_{R\rightarrow O} \rangle$) obtained from both QM and QM/MM simulations; treatment of noise encountered in the extreme edges of the initial distributions; discussion of the statistical uncertainties of each quantity; a graph displaying the difference in the solvent's structural reorganization upon singlet and triplet $[Ru(bpy)_3]^{2+}$ oxidation; and complete citations of references whose author lists had to be shortened because of their length. This material is available free of charge via the Internet at http://pubs.acs.org.

AUTHOR INFORMATION

Corresponding Author

*E-mail: ursula.roethlisberger@epfl.ch.

Present Address

[†]J.F.G.: Laboratory for Computational Molecular Design, École Polytechnique Fédérale de Lausanne, CH-1015 Lausanne, Switzerland.

Notes

The authors declare no competing financial interest.

■ ACKNOWLEDGMENTS

Swiss NSF Grants 200020-146645 and 200020-140865 and the NCCR-MUST interdisciplinary research program are acknowledged for funding. The authors thank the DIT/EPFL and the CSCS for computer time. We also thank Prof. Majed Chergui (EPFL Laboratory of Ultrafast Spectroscopy) for valuable discussions that strongly contributed to the present work.

■ REFERENCES

(1) Juris, A.; Balzani, V.; Barigelleti, F.; Campagna, S.; Belser, P.; Von Zelewsky, A. Ru(II) Polypyridine Complexes: Photophysics, Photochemistry, Electrochemistry, and Chemiluminescence. *Coord. Chem. Rev.* **1988**, *84*, 85−277.

(2) Campagna, S.; Puntoniero, F.; Nastasi, F.; Bergamini, G.; Balzani, V. Photochemistry and Photophysics of Coordination Compounds: Ruthenium. *Top. Curr. Chem.* **2007**, *280*, 117−214.

(3) Font, J.; de March, P.; Busque, F.; Casas, E.; Benitez, M.; Teruel, L.; Garcia, H. Periodic Mesoporous Silica Having Covalently Attached Tris(bipyridine)ruthenium Complex: Synthesis, Photovoltaic and Electrochemiluminescent Properties. *J. Mater. Chem.* **2007**, *17*, 2336−2343.

(4) Nazeeruddin, Md. K.; Klein, C.; Liska, P.; Grätzel, M. Synthesis of Novel Ruthenium Sensitizers and Their Application in Dye-Sensitized Solar Cells. *Coord. Chem. Rev.* **2005**, *249*, 1460−1467.

(5) Greenway, G. M.; Greenwood, A.; Watts, P.; Wiles, C. Solid-Supported Chemiluminescence and Electrogenerated Chemiluminescence Based on a Tris(2,2′-bipyridyl)ruthenium(II) Derivative. *Chem. Commun.* **2006**, 85−87.

(6) Gao, F. G.; Bard, A. J. Solid-State Organic Light-Emitting Diodes Based on Tris(2,2′-bipyridine)ruthenium(II) Complexes. *J. Am. Chem. Soc.* **2000**, *122*, 7426−7427.

(7) Bossmann, S. H.; Jockusch, S.; Schwarz, P.; Baumeister, B.; Gob, S.; Schnabel, C.; Paywan, L., Jr.; Pokhrel, M. R.; Worner, M.; Braun, A. M.; et al. Ruthenium(II)−tris-bipyridine/Titanium Dioxide Codoped Zeolite Y Photocatalysts: II. Photocatalyzed Degradation of the Model Pollutant 2,4-Xylidine, Evidence for Percolation Behavior. *Photochem. Photobiol. Sci.* **2003**, *2*, 477−486.

(8) Ogawa, M.; Balan, B.; Ajayakumar, G.; Masaoka, S.; Kraatz, H.-B.; Muramatsu, M.; Ito, S.; Nagasawa, Y.; Miyasaka, H.; Sakai, K. Photoinduced Electron Transfer in Tris(2,2′-bipyridine)ruthenium-(II)−Viologen Dyads with Peptide Backbones Leading to Long-Lived Charge Separation and Hydrogen Evolution. *Dalton Trans.* **2010**, *39*, 4421−4434.

(9) Takashima, H.; Fukuda, M.; Nakagaki, F.; Ogata, T.; Tsukahara, K. Photoinduced Electron-Transfer Reactions of Carbonic Anhydrase Inhibitor Containing Tris(2,2′-bipyridine)ruthenium(II) Analogue. *J. Phys. Chem. B* **2013**, *117*, 2625−2635.

(10) Ruggi, A.; Beekman, C.; Wasserberg, D.; Subramaniam, V.; Reinhoudt, D. N.; van Leeuwen, F. W. B.; Velders, A. H. Dendritic Ruthenium(II)-Based Dyes Tuneable for Diagnostic or Therapeutic Applications. *Chem.—Eur. J.* **2011**, *17*, 464−467.

(11) Navon, G.; Sutin, N. Mechanism of the Quenching of the Phosphorescence of Tris(2,2′-bipyridine)ruthenium(II) by Some Cobalt(III) and Ruthenium(III) Complexes. *Inorg. Chem.* **1974**, *13*, 2159−2164.

(12) Bertolesi, G. E.; Trigoso, C. I.; Espada, J.; Stockert, J. C. Cytochemical Application of Tris(2,2′-bipyridine)ruthenium(II): Fluorescence Reaction with Solvated Polyanions of Mast Cell Granules. *J. Histochem. Cytochem.* **1995**, *43*, 537−543.

(13) Gawelda, W.; Johnson, M.; de Groot, F. M. F.; Abela, R.; Bressler, C.; Chergui, M. Electronic and Molecular Structure of Photoexcited $[Ru^{II}(bpy)_3]^{2+}$ Probed by Picosecond X-ray Absorption Spectroscopy. *J. Am. Chem. Soc.* **2006**, *128*, 5001−5009.

(14) Seidel, R.; Faubel, M.; Winter, B.; Blumberger, J. Single-Ion Reorganization Free Energy of Aqueous $Ru(bpy)_3^{2+/3+}$ and $Ru(H_2O)_6^{2+/3+}$ from Photoemission Spectroscopy and Density Functional Molecular Dynamics Simulation. *J. Am. Chem. Soc.* **2009**, *131*, 16127−16137.

(15) Moret, M.-E.; Tavernelli, I.; Rothlisberger, U. Combined QM/MM and Classical Molecular Mechanics Study of $[Ru(bpy)_3]^{2+}$ in Water. *J. Phys. Chem. B* **2009**, *113*, 7737−7744.

(16) Moret, M.-E.; Tavernelli, I.; Chergui, M.; Rothlisberger, U. Electron Localization Dynamics in the Triplet Excited State of $[Ru(bpy)_3]^{2+}$ in Aqueous Solution. *Chem.—Eur. J.* **2010**, *16*, 5889−5894.

(17) Damrauer, N. H.; Cerullo, G.; Yeh, A.; Boussie, T. R.; Shank, C. V.; McCusker, J. K. Femtosecond Dynamics of Excited-State Evolution in $[Ru(bpy)_3]^{2+}$. *Science* **1997**, *275*, 54−57.

(18) Yeh, A.; Shank, C. V.; McCusker, J. K. Ultrafast Electron Localization Dynamics Following Photo-Induced Charge Transfer. *Science* **2000**, *289*, 935−938.

(19) Creutz, C.; Chou, M.; Netzel, T. L.; Okumura, M.; Sutin, N. Lifetimes, Spectra, and Quenching of the Excited States of Polypyridine Complexes of Iron(II), Ruthenium(II) and Osmium(II). *J. Am. Chem. Soc.* **1980**, *102*, 1309−1319.

(20) Sutin, N. Light-Induced Electron Transfer Reactions. *J. Photochem.* **1979**, *10*, 19−40.

(21) Lin, C. T.; Böttcher, W.; Chou, M.; Creutz, C.; Sutin, N. Mechanism of the Quenching of the Emission of Substituted Polypyridineruthenium(II) Complexes by Iron(III), Chromium(III), and Europium(III) Ions. *J. Am. Chem. Soc.* **1976**, *98*, 6536−6544.

(22) Brunschwig, B. S.; Creutz, C.; McCartney, D. H.; Sham, T. K.; Sutin, N. The Role of Inner-Sphere Configuration Changes in Electron-Exchange Reactions of Metal Complexes. *Faraday Discuss. Chem. Soc.* **1982**, *74*, 113−127.

(23) Rillema, D. P.; Jones, D. S.; Levy, H. A. Structure of Tris(2,2′-bipyridyl)ruthenium(II) Hexafluorophosphate $[Ru(bipy)_3][PF_6]_2$; X-ray Crystallographic Determination. *J. Chem. Soc., Chem. Commun.* **1979**, 849−851.

(24) Bühl, M.; Kabrede, H. Geometries of Transition-Metal Complexes from Density-Functional Theory. *J. Chem. Theory Comput.* **2006**, *2*, 1282−1290.

(25) Blumberger, J. Free Energies for Biological Electron Transfer from QM/MM Calculation: Method, Application and Critical Assessment. *Phys. Chem. Chem. Phys.* **2008**, *10*, 5651−5667.

(26) Warshel, A. Dynamics of Reactions in Polar Solvents. Semiclassical Trajectory Studies of Electron-Transfer and Proton-Transfer Reactions. *J. Phys. Chem.* **1982**, *86*, 2218−2224.

(27) King, G.; Warshel, A. Investigation of the Free Energy Functions on Electron Transfer Reactions. *J. Chem. Phys.* **1990**, *93*, 8682−8692.

(28) Tavernelli, I.; Vuilleumier, R.; Sprik, M. Ab-Initio Molecular Dynamics for Molecules with Variable Number of Electrons. *Phys. Rev. Lett.* **2002**, *88*, No. 213002.

(29) Blumberger, J.; Tavernelli, I.; Klein, M. L.; Sprik, M. Diabatic Free Energy Curves and Coordination Fluctuations for the Aqueous Ag^+/Ag^{2+} Redox Couple: A Biased Born−Oppenheimer Molecular Dynamics Investigation. *J. Chem. Phys* **2006**, *124*, No. 064507.

(30) Cascella, M.; Magistrato, A.; Tavernelli, I.; Carloni, P.; Rothlisberger, U. Role of Protein Frame and Solvent for the Redox Properties of Azurin from *Pseudomonas aeruginosa*. *Proc. Natl. Acad. Sci. U.S.A.* **2006**, *103*, 19641−19646.

(31) Sulpizi, M.; Raugei, S.; VandeVondele, J.; Carloni, P.; Sprik, M. Calculation of Redox Properties: Understanding Short- and Long-Range Effects in Rubredoxin. *J. Phys. Chem. B* **2007**, *111*, 3969−3976.

(32) Marcus, R. A. On The Theory of Oxidation−Reduction Reactions Involving Electron Transfer. I. *J. Chem. Phys.* **1956**, *24*, 966−978.

(33) Marcus, R. A. Electrostatic Free Energy and Other Properties of States Having Nonequilibrium Polarization. I. *J. Chem. Phys.* **1956**, *24*, 979−989.
(34) Marcus, R. A. On The Theory of Oxidation−Reduction Reactions Involving Electron Transfer. II. Applications to Data on the Rates of Isotopic Exchange Reactions. *J. Chem. Phys.* **1957**, *26*, 867−871.
(35) Marcus, R. A. On the Theory of Electron-Transfer Reactions. VI. Unified Treatment for Homogeneous and Electrode Reactions. *J. Chem. Phys.* **1965**, *43*, 679−701.
(36) Zwanzig, R. W. High-Temperature Equation of State by a Perturbation Method. I. Nonpolar Gases. *J. Chem. Phys.* **1954**, *22*, 1420−1426.
(37) Jorgensen, W. L.; Chandrasekhar, J.; Madura, J. D.; Impey, R. W.; Klein, M. L. Comparison of Simple Potential Functions for Simulating Liquid Water. *J. Chem. Phys.* **1983**, *79*, 926−935.
(38) Case, D. A.; Darden, T. A.; Cheatham, T. E., III; Simmerling, C. L.; Wang, J.; Duke, R. E.; Luo, R.; Walker, R. C.; Zhang, W.; Merz, K. M.; et al. *Amber 11*; University of California: San Francisco, 2010.
(39) Wang, J. M.; Wolf, R. M.; Caldwell, J. W.; Kollman, P. A.; Case, D. A. Development and Testing of a General Amber Force Field. *J. Comput. Chem.* **2004**, *25*, 1157−1174.
(40) Moret, M.-E. A QM/MM Study of the Optical and Excited State Properties of $[Ru(bpy)_3]^{2+}$ in Water. Diploma Thesis, EPFL, Lausanne, Switzerland, Feb 18, 2005.
(41) Car, R.; Parrinello, M. Unified Approach for Molecular Dynamics and Density-Functional Theory. *Phys. Rev. Lett.* **1985**, *55*, 2471−2474.
(42) The CPMD Consortium Page. http://www.cpmd.org (accessed March 18, 2014).
(43) Troullier, N.; Martins, J. L. Efficient Pseudopotentials for Plane-Wave Calculations. *Phys. Rev. B* **1991**, *43*, 1993−2006.
(44) Perdew, J. P. Density-Functional Approximation for the Correlation Energy of the Inhomogeneous Electron Gas. *Phys. Rev. B* **1986**, *33*, 8822−8824.
(45) Becke, A. D. Density-Functional Exchange-Energy Approximation with Correct Asymptotic Behavior. *Phys. Rev. A* **1988**, *38*, 3098−3100.
(46) van Gunsteren, W. F.; et al. *Biomolecular Simulation: The GROMOS96 Manual and User Guide*; vdf Hochschulverlag AG an der ETH Zürich: Zürich, Switzerland and BIOMOS b.v.: Groningen, The Netherlands, 2006.
(47) Laio, A.; VandeVondele, J.; Rothlisberger, U. A Hamiltonian Electrostatic Coupling Scheme for Hybrid Car−Parrinello Molecular Dynamics Simulations. *J. Chem. Phys.* **2002**, *116*, 6941−6947.
(48) Colombo, M. C.; Guidoni, L.; Laio, A.; Magistrato, A.; Maurer, P.; Piana, S.; Rohrig, U.; Spiegel, K.; Sulpizi, M.; VandeVondele, J.; et al. Hybrid QM/MM Car−Parrinello Simulations of Catalytic and Enzymatic Reactions. *Chimia* **2002**, *56*, 13−19.
(49) Frisch, M. J.; Trucks, G. W.; Schlegel, H. B.; Scuseria, G. E.; Robb, M. A.; Cheeseman, J. R.; Scalmani, G.; Barone, V.; Mennucci, B.; Petersson, G. A.; et al. *Gaussian 09*, revision A.1; Gaussian, Inc.: Wallingford, CT, 2009.
(50) Miertus, S.; Scrocco, E.; Tomasi, J. Electrostatic Interaction of a Solute with the Continuum. A Direct Utilization of ab Initio Molecular Potentials for the Prevision of Solvent Effects. *Chem. Phys.* **1981**, *55*, 117−129.
(51) Amovilli, C.; Barone, V.; Cammi, R.; Cances, E.; Cossi, M.; Mennucci, B.; Pomelli, C. S.; Tomasi, J. Recent Advances in the Description of Solvent Effects with the Polarizable Continuum Model. *Adv. Quantum Chem.* **1998**, *32*, 227−261.
(52) Tomasi, J.; Cammi, R.; Mennucci, B.; Cappelli, C. Molecular Properties in Solution Described with a Continuum Solvation Model. *Phys. Chem. Chem. Phys.* **2002**, *4*, 5697−5712.
(53) Cossi, M.; Barone, V. Solvent Effect on Vertical Electronic Transitions by the Polarizable Continuum Model. *J. Chem. Phys.* **2000**, *112*, 2427−2435.
(54) Cossi, M.; Barone, V. Separation between Fast and Slow Polarizations in Continuum Solvation Models. *J. Phys. Chem. A* **2000**, *104*, 10614−10622.
(55) Jagoda-Cwiklik, B.; Slavíček, P.; Cwiklik, L.; Nolting, D.; Winter, B.; Jungwirth, P. Ionization of Imidazole in the Gas Phase, Microhydrated Environments, and in Aqueous Solution. *J. Phys. Chem. A* **2008**, *112*, 3499−3505.
(56) Jagoda-Cwiklik, B.; Slavíček, P.; Nolting, D.; Winter, B.; Jungwirth, P. Ionization of Aqueous Cations: Photoelectron Spectroscopy and ab Initio Calculations of Protonated Imidazole. *J. Phys. Chem. B* **2008**, *112*, 7355−7358.
(57) Pluhařová, E.; Jungwirth, P.; Bradforth, S. E.; Slavíček, P. Ionization of Purine Tautomers in Nucleobases, Nucleosides, and Nucleotides: From the Gas Phase to the Aqueous Environment. *J. Phys. Chem. B* **2011**, *115*, 1294−1305.
(58) de Leeuw, S. W.; Perram, J. W.; Smith, E. R. Simulation of Electrostatic Systems in Periodic Boundary Conditions. I. Lattice Sums and Dielectric Constants. *Proc. R. Soc. A* **1980**, *373*, 27−56.
(59) Kleinman, L. Comment on the Average Potential of a Wigner Solid. *Phys. Rev. B* **1981**, *24*, 7412−7414.
(60) Asthagiri, D.; Pratt, L. R.; Ashbaugh, H. S. Absolute Hydration Free Energies of Ions, Ion−Water Clusters, and Quasichemical Theory. *J. Chem. Phys.* **2003**, *119*, 2702−2708.
(61) Adriaanse, C.; Sulpizi, M.; VandeVondele, J.; Sprik, M. The Electron Attachment Energy of the Aqueous Hydroxyl Radical Predicted from the Detachment Energy of the Aqueous Hydroxide Anion. *J. Am. Chem. Soc.* **2009**, *131*, 6046−6047.
(62) Tissandrier, M. D.; Cowen, K. A.; Feng, W. Y.; Gundlag, E.; Cohen, M. H.; Earhart, A. D.; Coe, J. V. The Proton's Absolute Aqueous Enthalpy and Gibbs Free Energy of Solvation from Cluster-Ion Solvation Data. *J. Phys. Chem. A* **1998**, *102*, 7787−7794.
(63) Sulpizi, M.; Sprik, M. Acidity Constants from Vertical Energy Gaps: Density Functional Theory Based Molecular Dynamics Implementation. *Phys. Chem. Chem. Phys.* **2008**, *10*, 5238−5249.
(64) Lee, C.; Yang, W.; Parr, R. G. Development of the Colle−Salvetti Correlation-Energy Formula into a Functional of the Electron Density. *Phys. Rev. B* **1988**, *37*, 785−789.
(65) Figueirido, F.; Del Buono, G. S.; Levy, R. M. On Finite-Size Effects in Computer Simulations Using the Ewald Potential. *J. Chem. Phys.* **1995**, *103*, 6133−6142.
(66) Roux, B.; Yu, H.-A.; Karplus, M. Molecular Basis for the Born Model of Ion Solvation. *J. Phys. Chem.* **1990**, *94*, 4683−4688.
(67) Chan, D. Y. C.; Mitchell, D. J.; Ninham, B. W. A Model of Solvent Structure around Ions. *J. Chem. Phys.* **1979**, *70*, 2946−2957.
(68) Zhao, Y.; Truhlar, D. G. A New Local Density Functional for Main-Group Thermochemistry, Transition Metal Bonding, Thermochemical Kinetics, and Noncovalent Interactions. *J. Chem. Phys.* **2006**, *125*, No. 194101.